Numerical Analyses on the Missile Impact Tests performed at VTT within the Benchmark Project IRIS

--

Modelling Approach & Preliminary Results

Oliver Martin[1] / Vincent Centro[2] / Thierry Schwoertzig[2]

[1] European Commission, Joint Research Centre – Institute for Energy
[2] Altair Engineering France

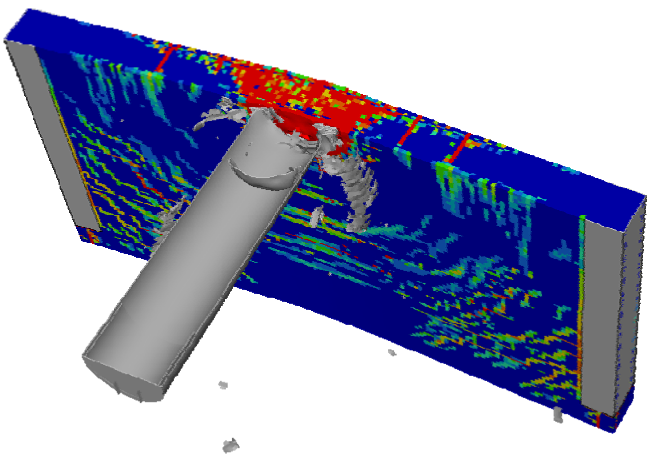

EUR 24880 EN - 2011

EUROPEAN COMMISSION

Institute for Energy

The mission of the JRC-IE is to provide support to Community policies related to both nuclear and non-nuclear energy in order to ensure sustainable, secure and efficient energy production, distribution and use.

European Commission
Joint Research Centre
Institute for Energy

Contact information
Address: Oliver Martin, JRC-IE, Westerduinweg 3, NL-1755 LE Petten
E-mail: oliver.martin@jrc.nl
Tel.: +31-224-56-5375
Fax: +31-224-56-5637

SPNR/POS/11 05 003

http://ie.jrc.ec.europa.eu/
http://www.jrc.ec.europa.eu/

Legal Notice
Neither the European Commission nor any person acting on behalf of the Commission is responsible for the use which might be made of this publication.

Europe Direct is a service to help you find answers to your questions about the European Union

Freephone number (*):

00 800 6 7 8 9 10 11

(*) Certain mobile telephone operators do not allow access to 00 800 numbers or these calls may be billed.

A great deal of additional information on the European Union is available on the Internet.
It can be accessed through the Europa server http://europa.eu/

JRC 65180

EUR 24880 EN
ISBN 978-92-79-20664-1
ISSN 1018-5593
doi:10.2790/3456

Luxembourg: Publications Office of the European Union

© European Union, 2011

Reproduction is authorised provided the source is acknowledged

Printed in The Netherlands

Content

1 Introduction

This report describes the modelling approach and preliminary results of the first numerical analyses of Joint Research Centre (JRC) and Altair Engineering France on the missile impact tests performed at VTT within the Benchmark Project "Improving the Robustness of Assessment Methodologies for Structures impacted by Missiles (IRIS)" organised within the Nuclear Energy Agency (NEA) of OECD. The objective of the IRIS Benchmark Project is to assess the state-of-the-art of numerical modelling of missile impacts on concrete containment structures of nuclear power plants (NPPs). First considerations on the safety of NPPs against aircraft impacts (or missile impacts in a broader sense) were made in the late 1960s / early 1970s well before the start of the construction phase of the majority of today's operating commercial nuclear power reactors. To quantitatively assess the effects of aircraft impacts on concrete containment buildings (CCBs) of NPPs, nuclear organisations around the world carried out missile impact tests in the 1970s, either on a laboratory scale or a larger scale. In these tests metallic missiles, either small projectiles in the range of a few decimetres (lab scale tests) or large steel pipes in the range of a few metres (large scale tests), were impacted against adequately sized reinforced concrete slabs. An example for laboratory scale tests are the missile impact tests of CEA/EDF (Gueraud et al., 1976). Large scale tests are most notably the Meppen Slab Tests (Jonas et al., 1979; Nachtsheim & Stangenberg, 1982; Nachtsheim & Stangenberg, 1983; Rüdiger & Riech, 1983) and the tests performed at Sandia National Laboratory (Sugano et al., 1993a, 1993b).

Before and in parallel to the above missile impact tests computational analyses were performed to predict the outcome of the tests and to generally develop computational methods to quantitatively assess the effects of possible missile impacts on concrete containment structures. Empirical formulas were introduced mainly to estimate the penetration depth of aircrafts or missiles into CCBs (a summary of common empirical formulas can be found in Li et al., 2005). Parallel to the development of empirical formulas first numerical analyses were performed using either the finite difference (FD) method or the finite element (FE) method (a description of both methods can be found in Bathe (1990)). Due to the computational limitations at that time the numerical models of these first analyses were rather coarse and a number of simplifications had to be made.

Today with the availability of supercomputers and adequate numerical codes the possibilities for performing numerical missile impact analyses are fare greater compared to 30 to 40 years ago. Thus the issue is gaining quite a level of considerable interest inside the nuclear community again. In 2009 the Nuclear Energy Agency (NEA) of OECD and the "Institut de Radioprotection et de Sûreté Nucléaire (IRSN)", France called for the above mentioned benchmark project IRIS. The benchmark project is carried out within the Subgroup on Concrete of the Working Group on the Integrity and Ageing of Components and Structures (IAGE) of the NEA. It started in January 2010 and will be finalized in December 2010. The aim of the benchmark project is to assess the state-of-the-art of numerical missile impact analyses on concrete structures and to formulate recommendations on the appropriate modelling of such impact problems. Comparison of different modelling approaches & methodologies and solvers is envisaged. Benchmarking is conducted on two missile impact tests recently performed at the Technical Research Centre of Finland VTT and on one of the tests of the Meppen Slab Tests. The JRC in Petten, the Netherlands, participates in the benchmark project together with a contractor, Altair Engineering France, Antony, France. This report describes the modelling approach for the FE analyses on the three tests and presents results of first preliminary FE analyses on the two missile impact tests performed at VTT. These first preliminary numerical analyses were performed with the explicit FE solver RADIOSS of Altair Engineering (2009). The aim of the preliminary FE analyses is solely to investigate if the generated FE models give physically meaningful results according to the characteristics of concrete slabs and missiles used in the two impact tests at VTT. An in-depth comparison between computational results and test results will be subject of different reports when the test results are distributed to the benchmark participants.

2 Failure Modes

When a missile impacts into a reinforced concrete slab there are in principal two overall failure modes, flexural failure and punching shear failure. Both failure modes are caused by the elastic-plastic response of the reinforced concrete slab due to the impact of the missile. Both failure modes are displayed in Figure 1.

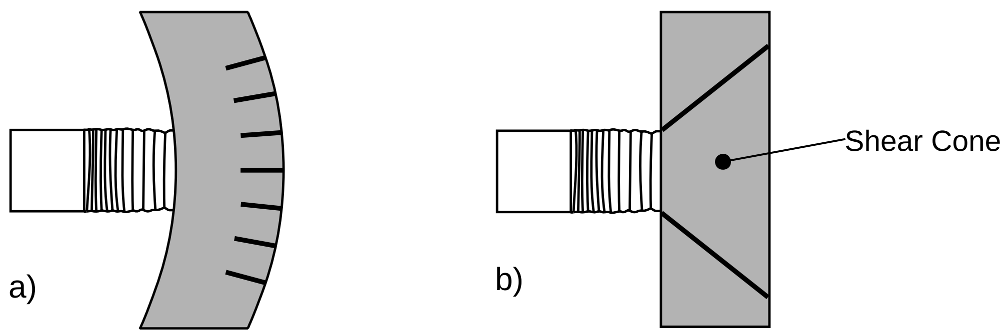

Fig. 1: a) Flexural failure and b) punching shear failure.

At the flexural failure mode the impact of the missile causes the reinforced concrete slab to bend. The front side of the concrete slab on which the missile impacts on (from now on referred to as the front side) undergoes compression loading. The back side of the concrete slab is subject to tension loading leading to the formation of cracks in thickness direction of the concrete slab. These cracks might penetrate deeply into the reinforced concrete slab and some scabbing (fall off) of concrete material on the back side of the slab might occur.

Normally, when a concrete slab is impacted by a missile, shear stresses occur inside the reinforced concrete slab. A so-called “shear cone” is formed. If the shear stresses are excessively high, considerable scabbing is likely to occur. Huge portions of concrete fall of the slab on its backside. In the worst case the shear cone is completely punched out of the reinforced concrete slab. This failure mechanism is called punching shear failure.

Whether flexural failure or punching shear is more likely to occur depends upon the design characteristics of the reinforced concrete slab and the missile. In case of a strong, dense reinforcement, flexural failure is more likely. In case of a weaker, less densely reinforcement and absence of any transversal reinforcement, punching shear failure becomes more likely. Soft missiles (pipes) tend to produce flexural failure, where as hard missiles tend to produce punching shear failure. Lower initial missile impact velocities promote flexural failure, where as high initial missile impact velocities promote punching shear failure. Also the thickness of the reinforced concrete slab plays a certain role. Flexural failure can only occur if the concrete slab is able to bend, which is only possible if it has a rather limited thickness compared to its height and width.

3 Missile Impact Tests used within the IRIS Benchmark Project

3.1 Overview of Tests and Reasons for their Usage

As mentioned in the Introduction the aim of the IRIS Benchmark Project is to assess the state-of-the-art of numerical missile impact analyses on concrete structures and to formulate recommendations on the appropriate modelling of such impact problems. Numerical analyses which are performed on a specific missile impact test should provide the likely failure mode and realistic result properties (deformation of slab and missile, energy balances, contact force between slab and missile, residual displacements, etc…) of the test according to the design characteristics of concrete slab and missile. Therefore three rather different missile impact tests were chosen within the IRIS Benchmark Project to perform numerical analyses on: two flexural failure tests and a punching shear failure test. The two flexural failure tests are one of the two tests performed at VTT (referred to as the VTT-IRSN Flexural Test) and the 4th test of the 2nd series of the Meppen Slab Tests (referred to as the Meppen II-4 Test). The punching shear test is the other missile impact test performed at VTT and is referred to as the VTT-CNSC-IRSN Punching Shear Test. According to the dimensions of the used reinforced concrete slabs both the VTT-IRSN Flexural Test and the VTT-CNSC-IRSN Punching Shear Test can still be considered as lab scale tests, where as the Meppen II-4 Test is a large scale test. Both the VTT-IRSN Flexural Test and the VTT-CNSC-IRSN Punching Shear Test are described more deeply in the next subchapter.

3.2 IRSN-VTT Flexural Test

In the VTT-IRSN Flexural Test a reinforced concrete slab of dimensions 2.1m $\times$ 2.1m $\times$ 0.15m is impacted by a soft missile. The concrete slab has longitudinal steel reinforcements at its front and back side and transverse reinforcement. All reinforcements are steel bars made of A500HW and have a unique diameter of 6mm. The density of the longitudinal reinforcements is 5 cm^2/m at front and back side and 50 cm^2/m^2 for the transverse reinforcement. The concrete slab is simply supported in a metallic frame as displayed in Figure 2.

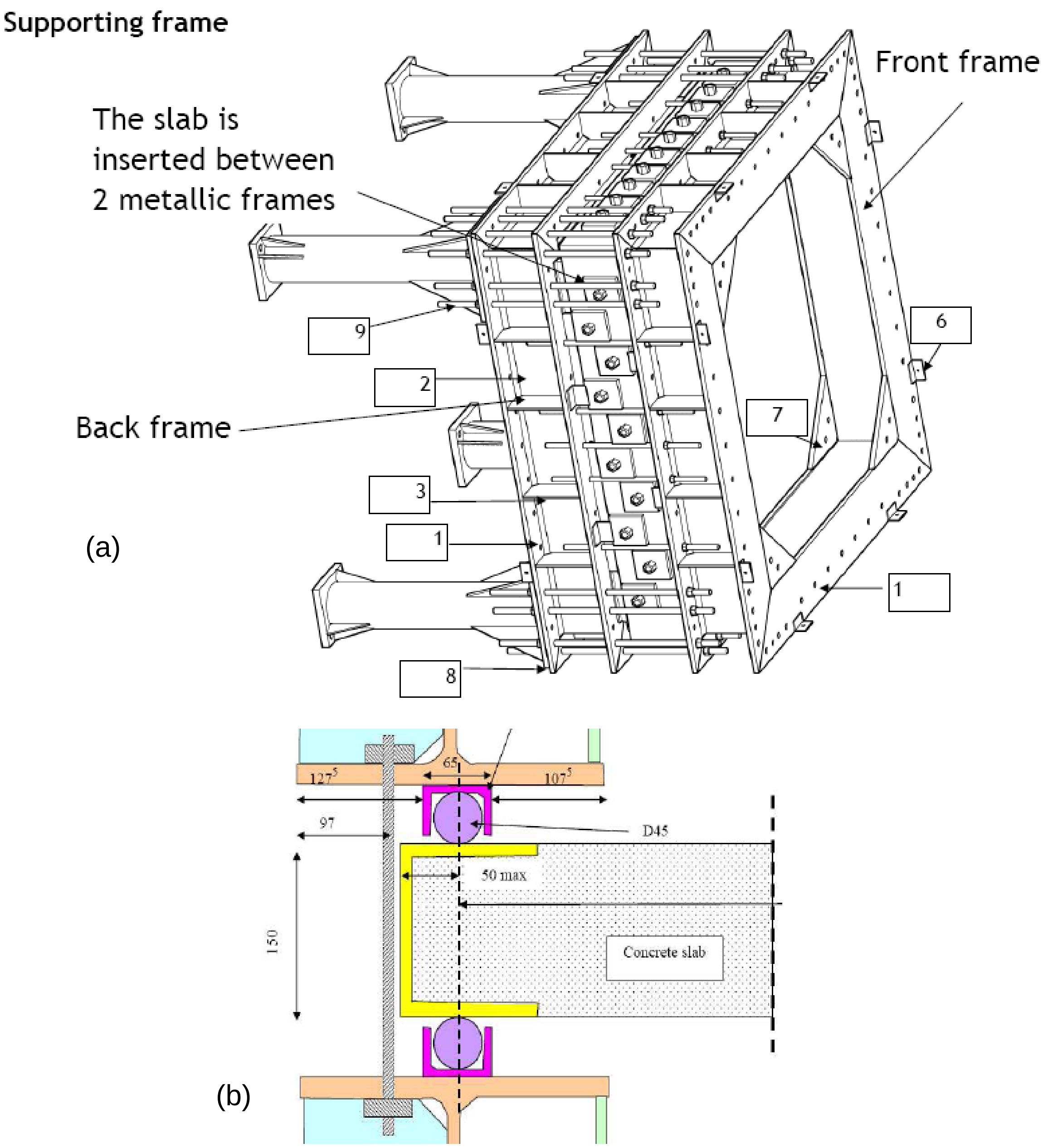

Fig. 2: Support of concrete slab during impact test: (a) Frame, (b) support (IRSN, 2010).

The missile used in the VTT-IRSN Flexural Test is basically a thin stainless steel (material: EN 1.4432) pipe of 2m length, 256mm outer diameter and 2mm thickness. The missile has a round shaped dome also of 2mm thickness and is made of the same material as the stainless steel pipe. At its rear the missile contains a short, more massive carbon steel pipe of 190mm length, 244.5mm diameter and 12.5mm thickness. The carbon steel pipe sits within the stainless steel pipe and both pipes are connected with screws. The missile is closed at its end with a massive carbon steel plate of 25mm thickness. Two rotation mitigators are fixed on the steel plate to avoid rotation of the missile around its main axis during the test. The missile has an overall mass of 50kg and an initial velocity of 110 m/s is envisaged. Figure 3 shows the design of the missile.

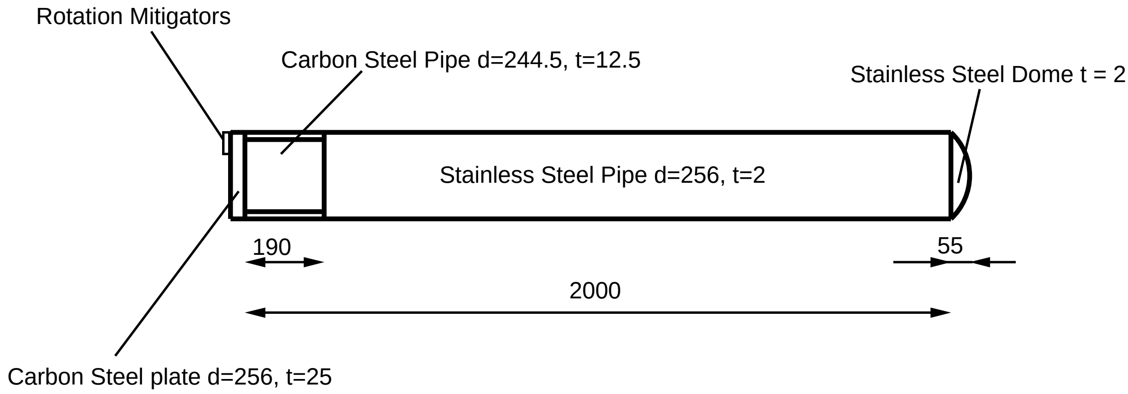

Fig. 3: Missile for the VTT-IRSN Flexural Test (IRSN, 2010).

3.3 IRSN-VTT-CNSC Punching Shear Test

In the VTT-CNSC-IRSN Punching Shear Test a thicker reinforced concrete slab (dimensions 2.1m × 2.1m × 0.25m) compared to the one in the VTT-IRSN Flexural Test is impacted by a hard missile. The concrete slab has longitudinal steel reinforcements at its front and back side and no transverse reinforcement. Again, the reinforcements are steel bars made of A500HW, but now have a diameter of 10mm. The density of the longitudinal reinforcements now is 8.7 cm^2/m at both sides and again the concrete slab is simply supported in the metallic frame as displayed in Figure 2.

The missile used in the VTT-CNSC-IRSN Punching Shear Test is a steel pipe of 580mm length, 168.3mm diameter and 10mm thickness filled with light-weight concrete. The missile has a massive round shaped steel dome (material: Fe52) with a thickness ranging from 30-50mm. The missile is closed at its end with a steel plate (material: Fe52) of 10mm thickness. A thin-walled aluminium pipe is fixed on the outer surface of the steel plate for determination of the residual velocity. The missile has an overall mass of 47kg and an initial velocity of 120 m/s is envisaged. Figure 4 shows the design of the missile.

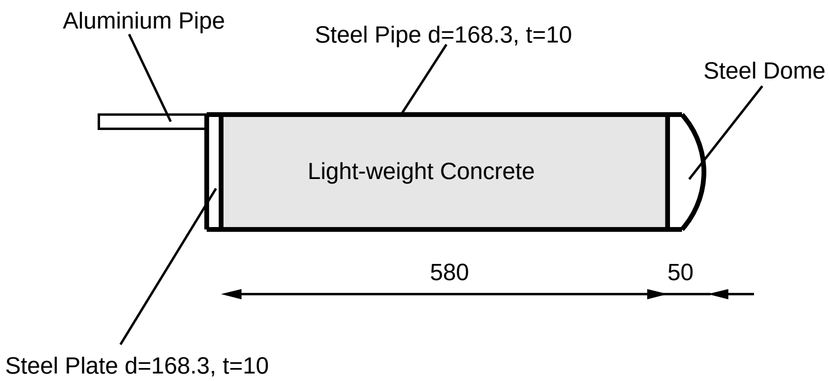

Fig. 4: Missile for the VTT-CNSC-IRSN Punching Shear Test (IRSN, 2010).

4 Finite Element Modelling Approach

4.1 FE Meshes

4.1.1 FE Meshes of the Concrete Slabs

Three dimensional (3D) Lagrangian meshes are used for the slabs and missiles of both tests. The FE models are complete models, so no symmetry conditions are used. The concrete is modelled with linear hexahedron elements of reduced integration, the eight noded BRICK element of RADIOSS. Viscous hourglass formulation is enabled together with geometric non-linearities and co-rotational formulation in order to ensure accurate response of the FE model with regards to the expected large deformations. The artificial bulk viscosity is set to zero in order to avoid numerical damping and is not needed since the missile velocities are in the subsonic range. The steel reinforcements are modelled with linear beam elements with proper inertia and cross section definitions. The nodes of the beam elements are merged with the nodes of the brick elements of the concrete. The bearing surfaces of the slab at the edges to the slab support are modelled with four noded shell elements of reduced integration. Their nodes are merged with the nodes of the underlying brick elements for the concrete.

Figure 5 shows the mesh for the slab of the VTT-IRSN Flexural Test. The mesh for the slab of the VTT-CNSC-IRSN Punching Shear Test looks similar. An average element size of 15mm is chosen for the meshes of both slabs, giving 13 elements in thickness direction for the model of the slab of the VTT-IRSN Flexural Test and 18 elements for the model of the slab of the VTT-CNSC-IRSN Punching Shear Test. This element refinement in thickness direction of the models of the slabs are seen as necessary in view of the slab dimensions and the reinforcement complexity in order to give sufficient accuracy. Smaller element sizes are required for those brick elements that are attached to the beam elements for the reinforcement to ensure uniform distances between neighbouring rebars. Table 1 provides the basic properties for the meshes of the two slabs.

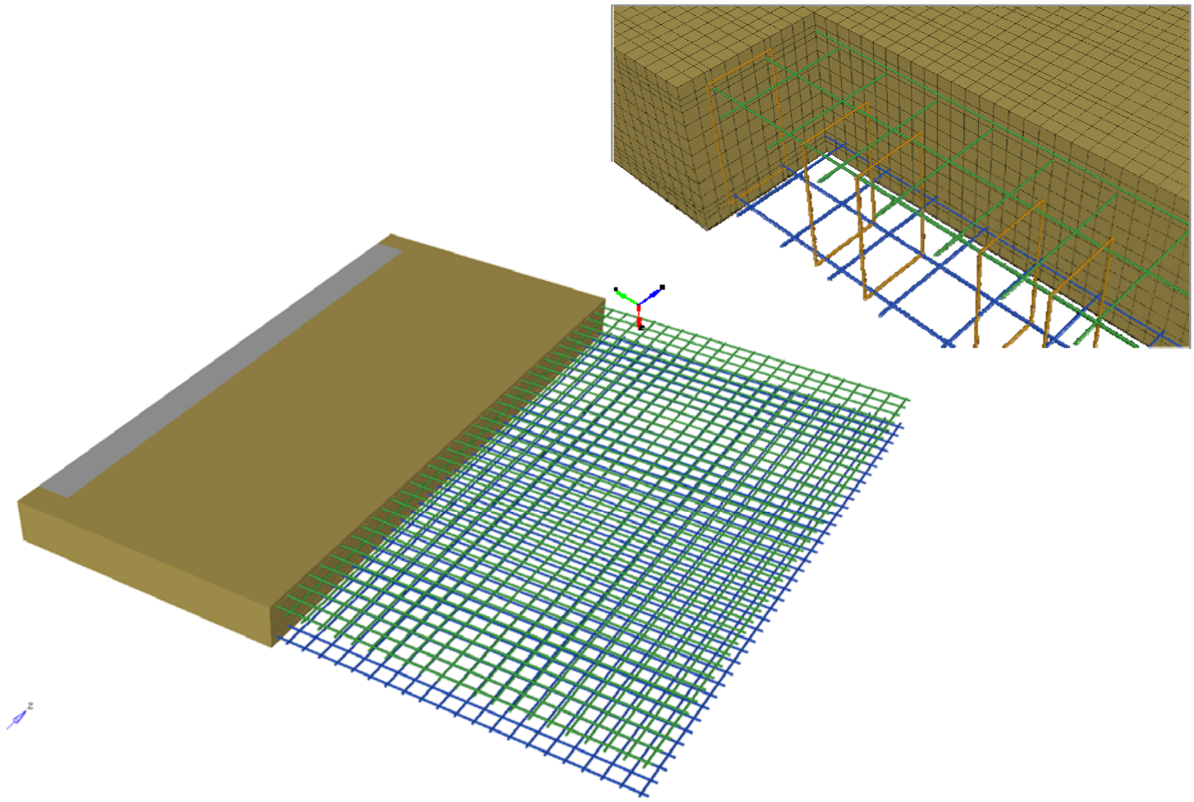

Fig. 5: Modelling approach and mesh for the concrete slab.

Table 1: Mesh properties of the slabs.

	VTT-IRSN Flexural	VTT-CNSC-IRSN Punching Shear
Element size [mm] Average Around rebars	 15 6	 15 10
No. elements in slab thickness	13	18
No. elements in total Brick (3D) Beam (1D) Shell (2D)	 351728 35384 9586	 304200 11776 8008
No. nodes	383418	326059

4.1.2 FE Meshes of the Missiles

All the thin-walled parts of the missiles (piping sections, plates of limited thickness) are modelled predominantly with four noded shell elements of reduced integration with a few three noded shell elements when necessary. Hourglass physical stabilisation is enabled to avoid unnecessary build-up of hourglass energy during the analyses. Massive sections of the missile for the VTT-CNSC-IRSN Punching Shear Test, i.e. dome and light-weigh-concrete filling, are modelled with eight noded brick elements of reduced integration. Figure 6 shows the FE meshes for both missiles and Table 2 provides the basic mesh properties.

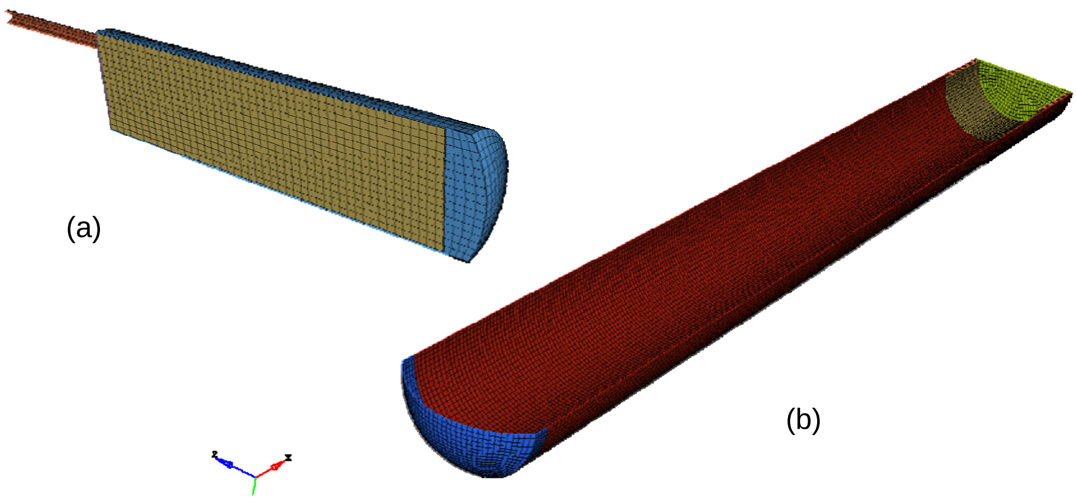

Fig. 6: FE models of the missiles for (a) VTT-CNSC-IRSN Punching Shear Test and (b) VTT-IRSN Flexural Test.

Table 2: Mesh properties of the missiles.

	VTT-IRSN Flexural	VTT-CNSC-IRSN Punching Shear
Average Element size [mm]	8	11
No. elements in total Shell (2D) Brick (3D)	 29820 0	 2796 11760
No. nodes	29934	16252

4.2 Constitutive Models

4.2.1 Constitutive Model for Concrete

The constitutive behaviour of the concrete is modelled with the non-uniform hardening plasticity model of Han and Chen (1985). It is a Drucker-Prager/Cap model and was designed to model the constitutive behaviour of reinforced concrete under dynamic impact loading. The material model of Han and Chen is characterised by a tri-axial open failure envelope with a closed yield envelope (cap) inside. Both are displayed in Figure 7. The material model allows anisotropic plasticity and hardening, where as the underlying hardening rule is non-uniform. Behaviour in tension and compression are different, which is characteristic for concrete. Failure is achieved either by tensile cracking (brittle fracture) or compressive crushing. The material model of Han and Chen accounts for opening and closure of cracks and sensitivity of shear stresses towards different states of compression (pressure sensitivity). It also accounts for volumetric dilatation under compression.

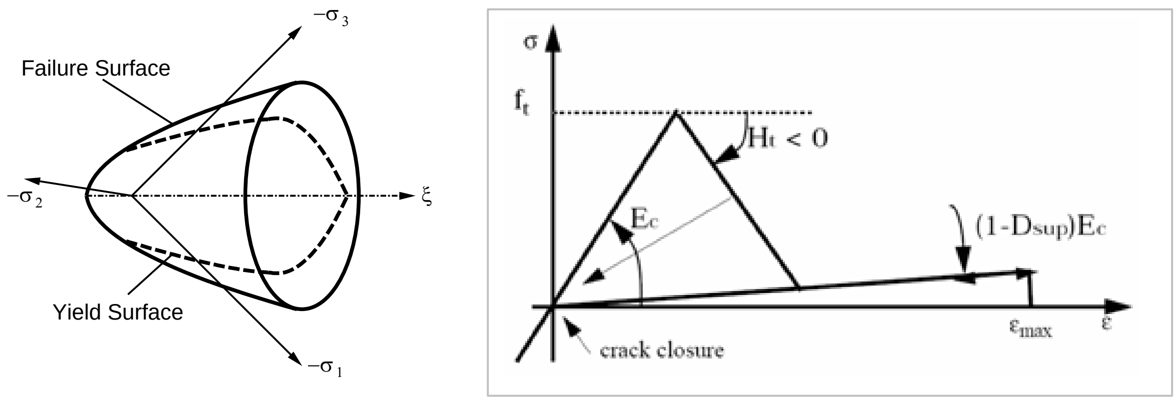

Fig. 7: The constitutive model for concrete of Han & Chen (1985): (a) Failure & yield envelopes, (b) stress-strain-curve in the tension regime.

The material model of Han and Chan is the standard material model for pre-stressed concrete in RADIOSS (material model no. 24 in RADIOSS) and in principle 21 parameters are necessary to fully describe the material model. In standard uni-axial material tests normally only a limited number of basic material parameters are determined, e.g. Young's modulus, compressive strength, etc… The implementation of the material model of Han and Chan in RADIOSS allows complete description of the model with just five basic material parameters. These are the initial mass density ρ, Youngs's modulus E, Poisson ratio ν, compression strength F_c and tensile tangent modulus H_t. The remaining material parameters are calculated from these five via default ratios between them or by taking default values. This is also the adopted approach for the FE analyses that are subject to this report.

A critical issue in any material model for concrete is the modelling of the energy release during crack propagation. This has significant impact in representing the damage evolution of the structure. The tensile damage behaviour is dependent on the cracking and post-cracking property, which itself is given by the tensile tangent modulus H_t (see Figure 7). It represents the tension stiffness when the concrete starts to crack, which is typically the case when the tensile strength is reached. With further increasing strain the stress decreases to a certain level, the residual stress level. The latter is provided by the maximum damage ratio D_{sup} (see Figure 7), which is normally set to a value close to one.

In the beginning of IRIS the following three material properties for the concrete were distributed to the benchmark participants only: Young's modulus E, compressive strength F_c and the tensile splitting strength F_{st}. Thus assumptions have to be made about the main missing material properties, in particular for the concrete tensile behaviour. The tensile strength F_t is assumed to be 10% of the compressive strength F_c. Experience shows that this is a reasonable assumption and a value of 0.1 is also the default ratio between the two properties in RADIOSS.

The tensile strength F_t is usually determined in a tensile splitting test, also known as the Brazilian test (Lacy et al., 2008), via the tensile splitting strength F_{st} (normally $F_t \neq F_{st}$). The principle of the test is displayed in Figure 8. A cylindrical test specimen is loaded locally on its outer surface with a pressure p until failure occurs. The tensile splitting strength F_{st} is then determined via Relationship (1). For a fixed tensile strength F_t (e.g. 10% of the compressive strength F_c) the failure load p may be used to calibrate the crack energy E_f in Equation (2) by adjusting the tensile tangent modulus H_t.

$$F_{st} = \frac{2p}{\pi l D} \qquad (1)$$

$$E_f = \frac{F_t^2}{2E} + \frac{F_t^2}{2H_t} \qquad (2)$$

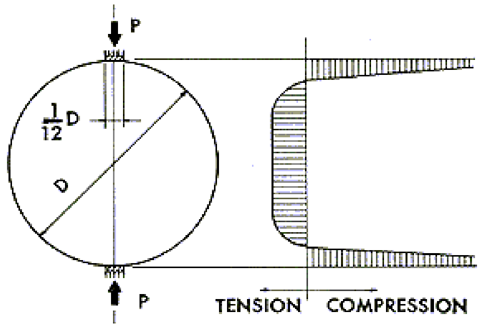

Fig. 8: Brazilian Test (Lacy et al., 2008).

With the material properties distributed to the benchmark participants the stress-strain curve in Figure 9 was produced. This is the one, which is used for all the analyses that are subject to this report. The values for all 21 material parameters are listed in Table A1 in the Appendix. RADIOSS allows the use of the described constitutive model for concrete in conjunction with an erosion law. This is a brittle failure criterion in tension that allows the removal of cracked (seriously damaged) elements from the model when a certain failure strain value is reached. This option is used for the FE analyses on the VTT-CNSC-IRSN Punching Shear Test, since significant scabbing of concrete is expected. The failure strain is set to the high value of 50% for the brick elements on the backside of the slab mesh.

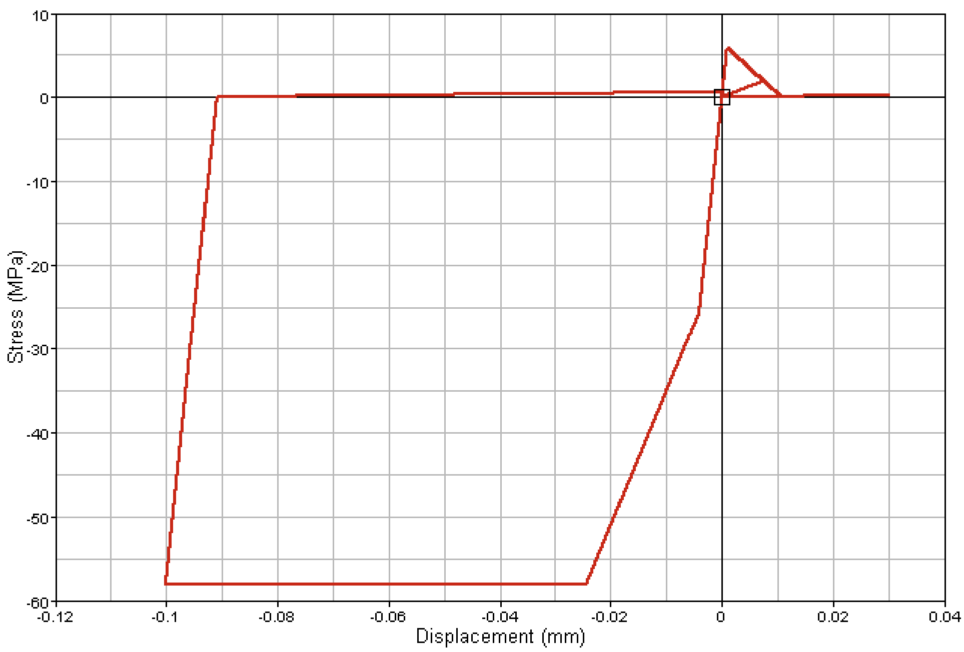

Fig. 9: Stress-strain curve used for the concrete including tension and compression regime.

For the brick elements attached to the beam elements for the reinfrocements a different tensile strength value is chosen, which is four times the regular value. The reason for this is indicated in Figure 10. The reinforcements inside the real concrete slabs occupy a certain volume. In the FE models the reinforcements are modelled with beam elements, which do not take away volume of the brick elements resembling the concrete. The consequence is an overestimation of the concrete in the FE models that could lead to an unrealistic build-up of crack energy. In order to avoid that the tensile strength for the brick elements, representing the concrete around the reinforcements as indicated in Figure 10, is raised compared to the other brick elements. Experience has shown that a factor of 4 has proved to be adequate.

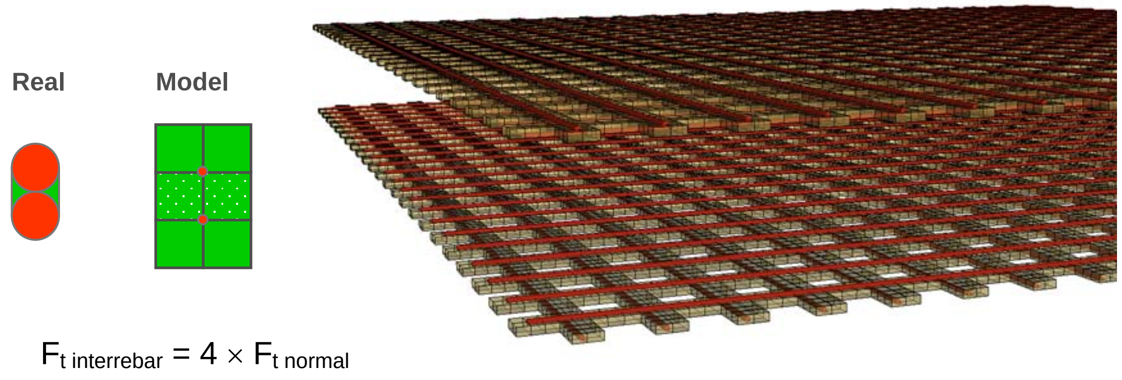

Fig. 10: Adjustment of tensile strength for brick elements around rebars to limit build up of crack energy.

4.2.2 Constitutive Model for the Steel Reinforcement

For the steel reinforcement isotropic elastic-plastic deformation with strain hardening is assumed. The hardening behaviour is defined via a Johnson-Cook model (RADIOSS Material model no. 2). Identical hardening curves are assumed for tension and compression. The Johnson-Cook model parameters are derived from the stress-strain curves displayed on the data sheets for the tests distributed to the benchmark participants (IRSN, 2010). No strain-rate effects are taken into account, because of lack of appropriate data and because they are seen as being of minor importance for the reinforcement (compared to the missile in the VTT-IRSN Flexural Test). In order to avoid continuous growth of stresses in the beam elements, representing the reinforcement, beyond the necking point of the involved material a maximum stress level for the beam elements is set to σ_{max} = 0.7 GPa. This value is a realistic assumption for the stress level for necking to start for the involved reinforcement material. The alternative of removing beam elements throughout the analyses when a certain stress level is reached is not used in order to avoid a weaker post-failure behaviour in the interactions between concrete-reinforcement and missile-reinforcement. Pre-stressing of reinforcement is not considered, because previous experience has shown that it has negligible effects on the analyses results (common conclusion of JRC and Altair Engineering France based on different, previous FE analyses). Table A2 in the appendix lists all the material parameters for the reinforcement in the FE models of the two impact tests. The same material properties are also used for the shell elements representing the metallic bearing surfaces of the slabs.

4.2.3 Constitutive Model for the Missiles

Also for the metallic parts of the missiles isotropic elastic-plastic deformation behaviour with strain hardening is assumed. For the stainless steel parts (main pipe and end cap) of the missile in the VTT-IRSN Flexural Test, a tabular function (RADIOSS material model no. 36) is used to describe the elastic-plastic behaviour of these sections. The tabular function is derived from the experimental stress-strain curve provided on the datasheet for the test that was distributed to the benchmark participants. Strain-rate effects in the deformation behaviour of the stainless steel sections are “weakly” considered by applying a scale factor to the basic stress-strain curve (= curve at strain-rate zero). The applied scale factor is 1.01 and corresponds to the high strain-rate value of 10^8 s^{-1}. In the tension regime a linear damage model is included in the constitutive model for the stainless steel as indicated in Figure 11. In the compression regime a maximum plastic strain ε_{max} is set in order to account for possible rupture in compression of the missile.

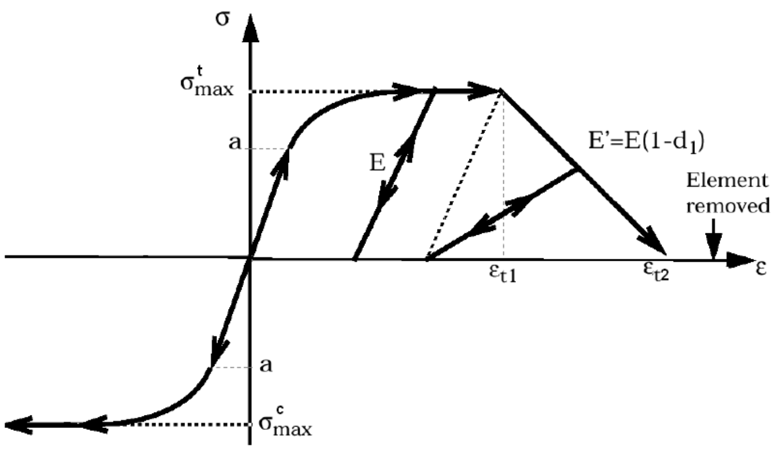

Fig. 11: Stress-strain curve with linear damage model in the tensile regime.

The constitutive behaviour of the carbon steel parts of the missile (carbon steel pipe and carbon steel plate) is described with a Johnson-Cook model. The Johnson-Cook model is generally favoured for ductile materials like carbon steels instead of tabular functions. Strain-rate dependencies are not considered for the carbon steel sections, since they are at the rear of the missile, where deformations are expected to be extremely limited. Maximum stress and strain values are set for the carbon steel sections. The mass densities of all four section meshes of the missile are adjusted so that the mass of each section mesh matches with the information provided on the data sheet for the test.

For all the metallic sections of the missile of the VTT-CNSC-IRSN Punching Shear Tests, which are steel pipe, dome, rear plate and aluminium pipe Johnson-Cook models are used to describe their elastic-plastic deformation behaviour. For steel pipe, dome and rear plate the same material parameters are used. They are extracted from stress-strain curves in literature. Linear tensile damage models as displayed in Figure 11 are included in the material models for the steel pipe and rear plate. Maximum stress and strain values are set for all four metallic parts as outlined before for the missile of the VTT-IRSN Flexural Test and the reinforcements. The mass densities of the metallic parts are adjusted so that the masses of their meshes correspond to the masses of the individual sections of the real missile. For the light-weight concrete filling of the missile the same material parameters are taken as for the concrete slab, except that the mass density is reduced, so that the overall mass of the FE model of the missile agrees with the mass of the real missile used in the test (see Table A1 in the Appendix). Tables A3 to A7 in the Appendix list all the material properties used for the models of the missiles.

4.3 Boundary Conditions and Contact Modelling

The concrete slabs are assumed to be simply supported along its vertical edges as indicated in Figure 12, but this might change when the tests are conducted (eventually the slabs are supported along all four edges).

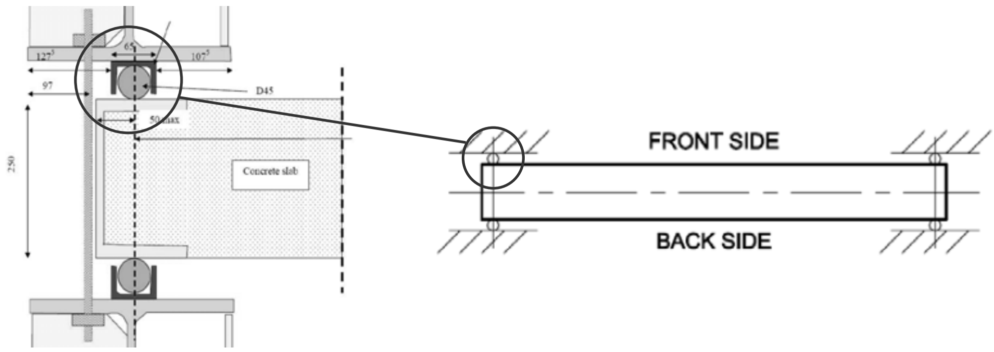

Fig. 12: Assumed slab support.

The interaction between concrete slab and supporting frame is modelled by defining stripes of moving rigid walls along the supporting edges of the slab on each side (see Figure 13). Kinematic contacts are defined between nodes on the bearing surfaces and the rigid wall stripes. This approach provides flexibility in the boundary conditions without imposing too harsh conditions (i.e. clamped nodes). Additionally, the rigid wall stripes are connected to springs in order to add damping and transversal deformation of the global steel fame (elongation ~1mm). The stiffness of the springs is adjusted according the impact conditions.

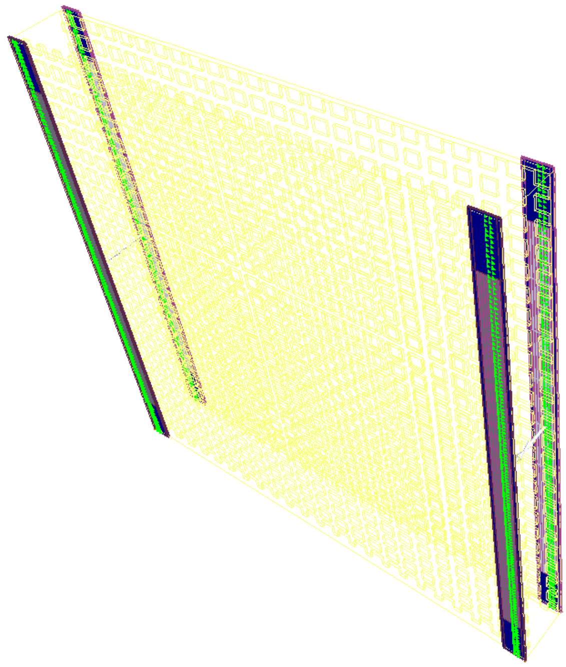

Fig. 13: Modelling approach slab support with moving rigid walls (green nodes are constrained nodes).

A general contact algorithm based on the penalty method is used for the interaction between missile and concrete slab. The contact domains are defined by specifying the master surface and slave nodes. The master surface contains all exterior element faces of the brick elements representing the concrete in the FE models of the two missile impact tests. The contact gap is set to half of the thickness of the average shell size of the mesh of the corresponding missile. The interface stiffness is automatically computed based on the softer characteristics between the master and slave surface with a minimum stiffness set to 1kN/mm. Possible interactions between beam elements of the reinforcements are considered via edge-to-edge contacts. The initial gap for these contacts is set to the sum of the rebar radius's in interaction. All contacts are assumed to be friction free, i.e. Coulomb friction is neglected. Self-contact for the missile is considered in the models. Removal of ruptured elements from interfaces is activated to prevent nodes connected to these deleted elements to impact with high velocities. Another set of self-contact is included in all the models encompassing the first layers of solid elements on the front side of each slab. This additional set of self-contact is needed in order to limit large compressive distortions of elements located in the impact zone. The self-contact gap is set to a value corresponding to 1/10 of the average brick element size.

The FE models of the missile are subject to initial velocities of 110m/s and 120 m/s for the VTT-IRSN Flexural Test and the VTT-CNSC-IRSN Punching Shear Test respectively (see Chapter 3). But prior to the actual analysis on the two impact tests some preliminary analyses are carried out. In these the FE models of the two missiles are each impacted against a rigid wall in order to validate the overall quality of the models and the feasibility of the expected failure modes. The pre-analyses also provide an estimate for the duration of the actual FE analyses on the two missile impact tests.

5 Results

5.1 Results for the VTT-IRSN Flexural Test

Figure 14 shows the simulated missile impact process at the beginning, after 5ms and after 10ms. The missile is crushed considerably (50% of its initial length), which is physically sound for impact problems where a soft missile made of a more brittle material impacts into a far stiffer structure. A slight deflection of the slab is also visible in Figure 14 and becomes more apparent later on when the results for the slab are discussed in more detail (see Figure 19).

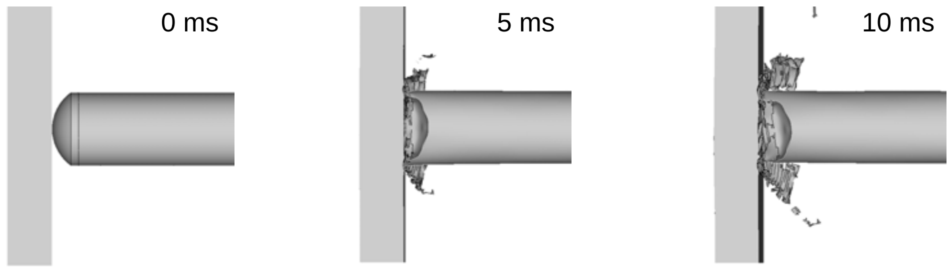

Fig. 14: Simulated impact process VTT-IRSN Flexural Test.

The physically soundness of the analysis is also supported by the energy balance, which is displayed in Figure 15. The initial kinetic energy of the missile is completely transformed into internal energy (deformation + damage energy) of slab and missile. The hourglass energy is negligible indicating that the analysis ran smoothly from a numerical point of view.

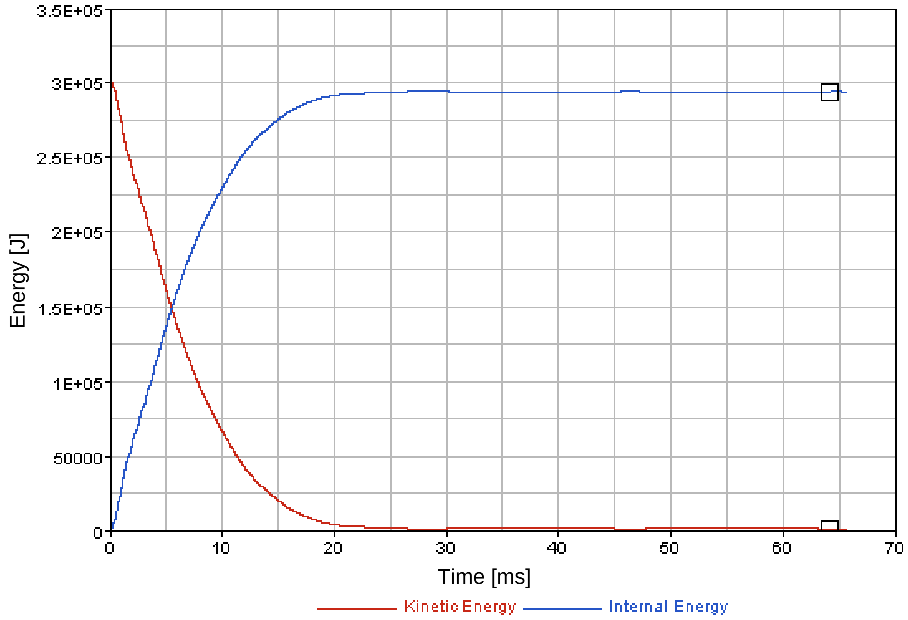

Fig. 15: Energy balance for the numerical analysis of the VTT-IRSN Flexural Test.

Figure 16 shows the contact force versus time between missile and slab. The contact force oscillates significantly in the beginning, but stabilizes and decreases to zero throughout the simulated impact process. The calculated duration of the impact process is 22 ms and the velocity of the missile is reduced completely to zero as shown in Figure 17. The flight direction of the missile is reversed and it moves back with a small velocity after the impact.

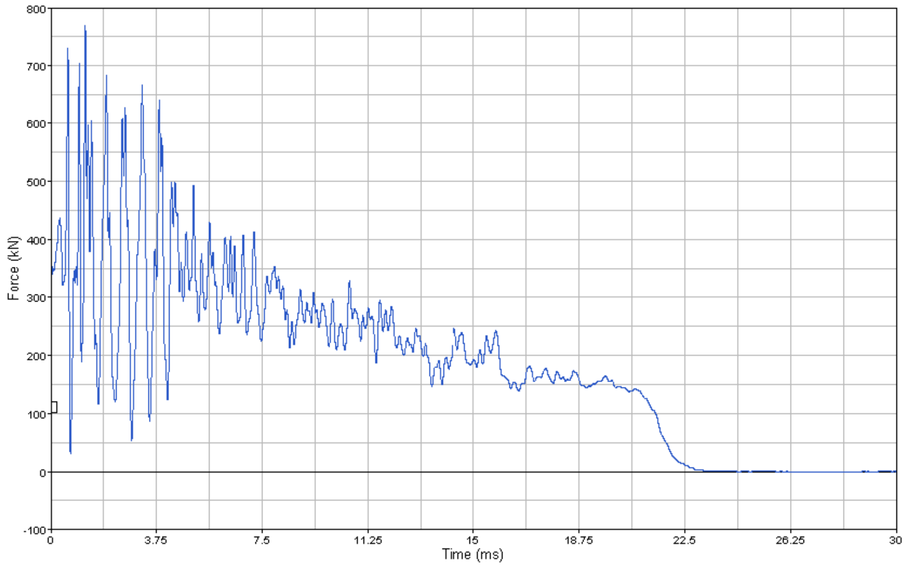

Fig. 16: Contact force versus time between missile and slab.

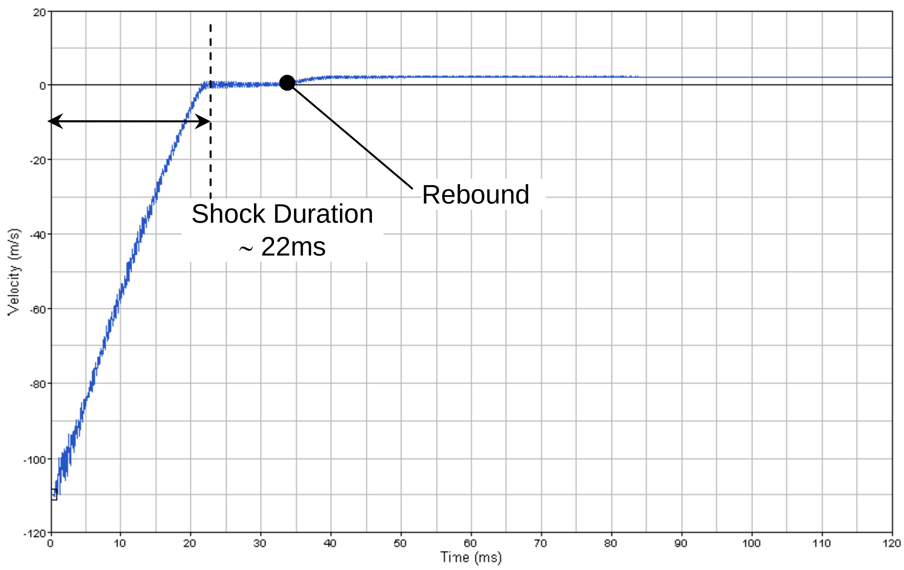

Fig. 17: Missile velocity versus time.

Figure 18 shows the damage pattern on the front and back side of the reinforced concrete slab after 30ms. Red areas indicate regions of high damage (cracked material). The displayed crack pattern is typical for a flexural failure test. Figure 19 shows the crack pattern inside the concrete slab. The pattern reveals the typical shear cone which always develops when a reinforced concrete slab is impacted by a missile (as previously mentioned in Chapter 2).

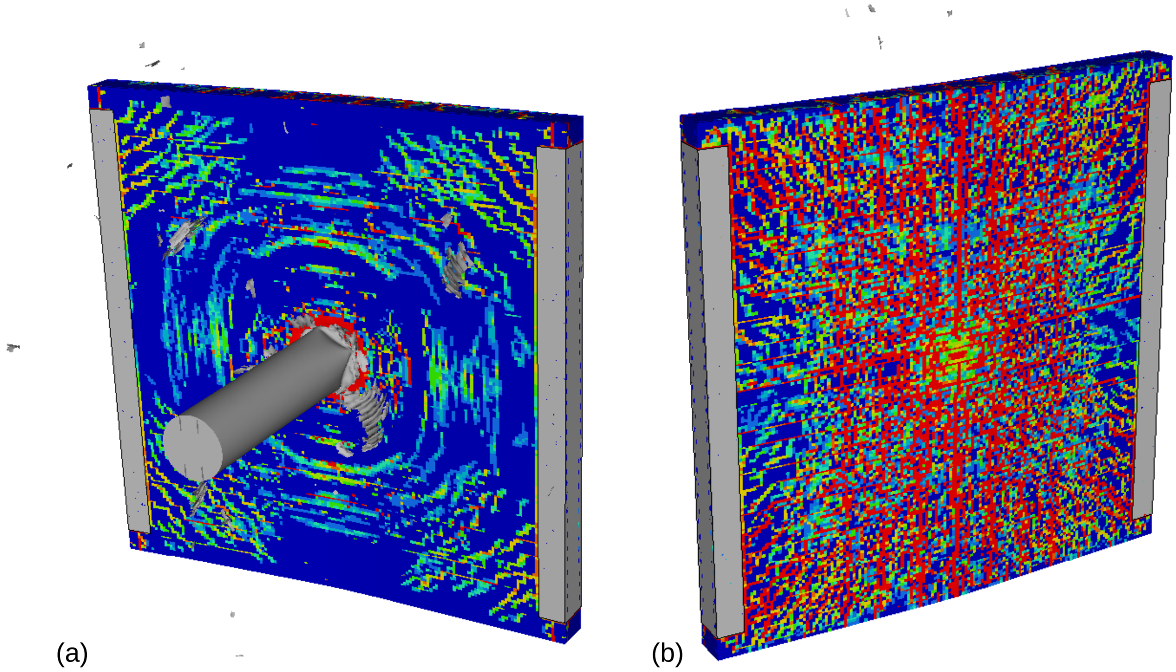

Fig. 18: Damage of the reinforced concrete slab after 30ms: (a) front side, (b) back side.

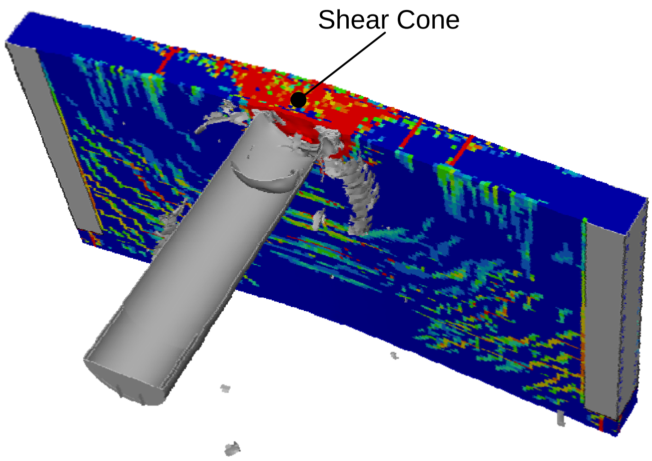

Fig. 19: Damage inside the reinforced concrete slab after 30ms.

Figure 20 shows the displacements versus time for various positions on the concrete slab. The displacements indicate considerable vibrations of the slab which always occur in a flexural test. The representation of slab vibrations in FE analyses on missile impact problems is normally one of the most challenging tasks.

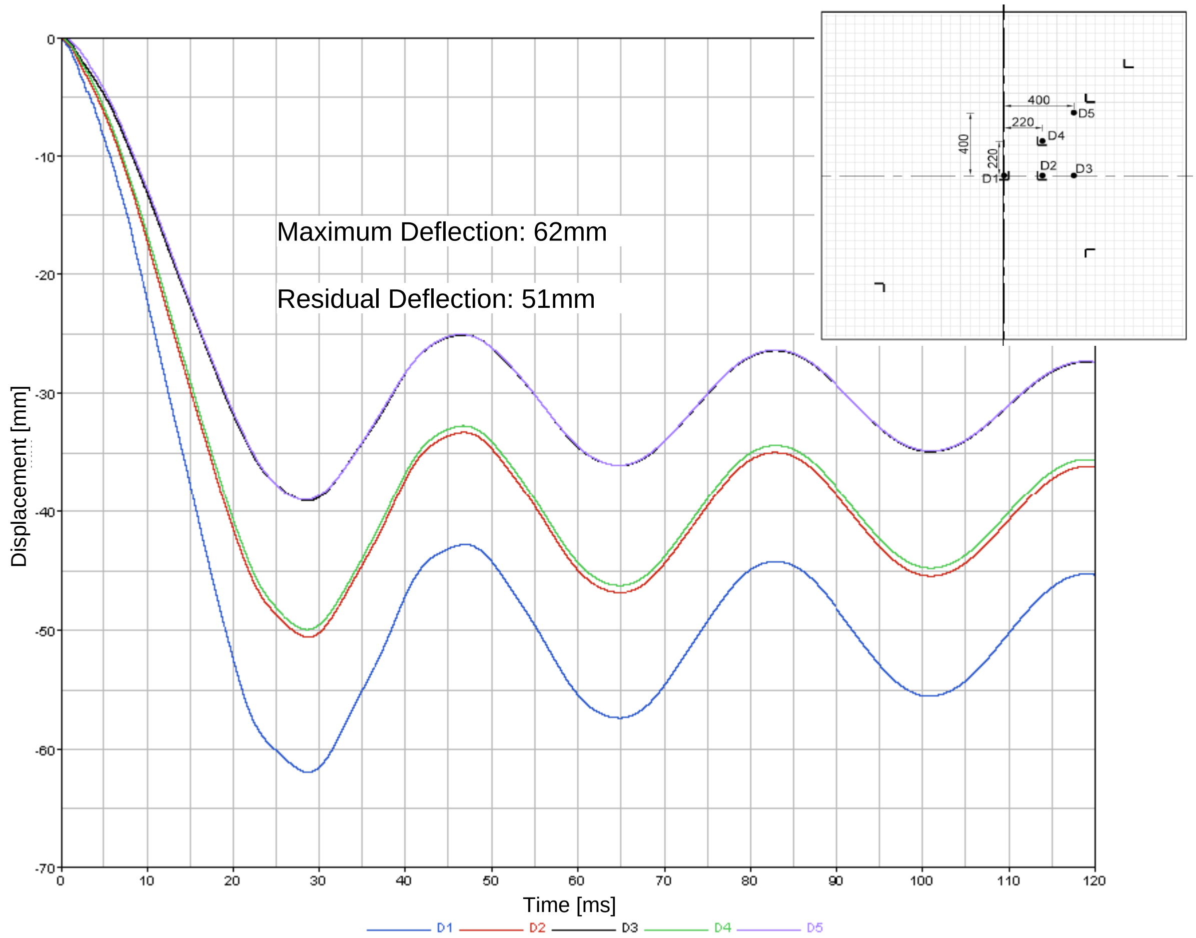

Fig. 20: Displacement versus time for various positions on the concrete slab.

Figure 21 shows the calculated strains for certain positions on the reinforcement. They also clearly display the vibration of the slab. Figure 21 also shows that the strain level of the reinforcement is the highest in the centre position of the slab (= missile impact location) and decreases to its edges. This result is in accordance with experience from missile impact tests.

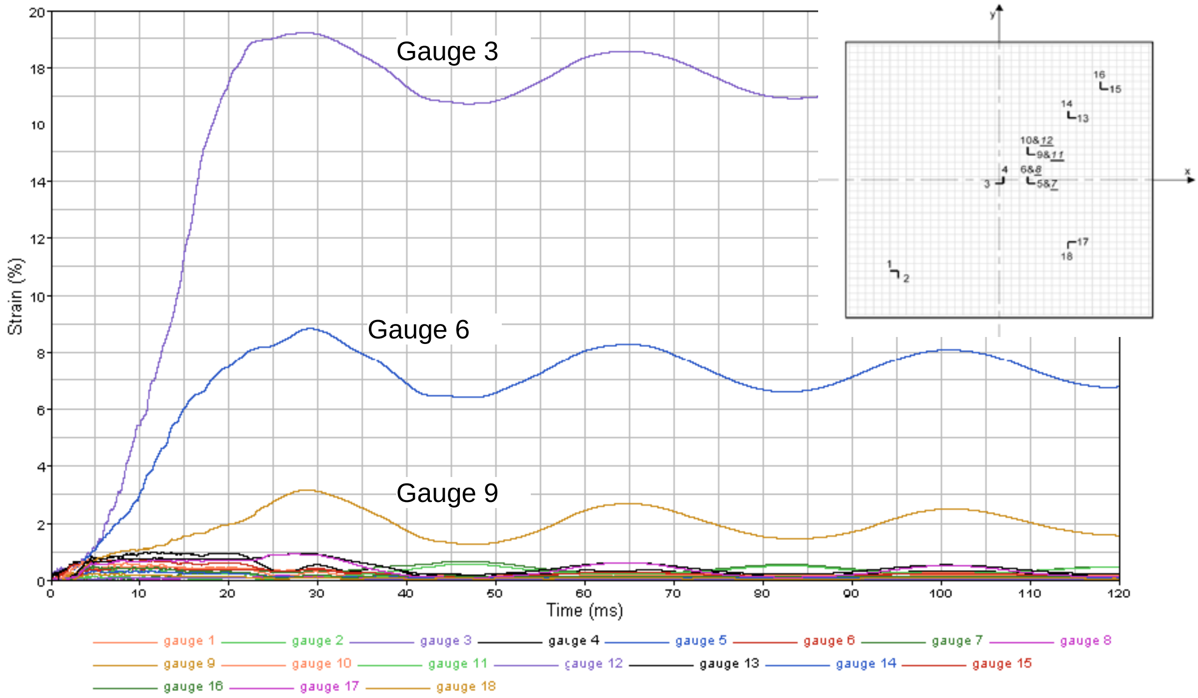

Fig. 21: Strains versus time for various positions on the reinforcement of the concrete slab.

5.2 Preliminary Results for the VTT-CNSC-IRSN Punching Shear Test

Figure 22 shows the energy balance for the VTT-CNSC-IRSN Punching Shear Test. In contrast to the VTT-IRSN Flexural Test the impact is “harder”, i.e. the transfer of the initial kinetic energy of the missile into deformation energy takes place in a much shorter time (less than 10ms). This is typical for missile impacts involving hard missiles. Figure 23 shows the contact force versus time between missile and slab. The contact force fluctuates only slightly in the beginning, indicating only little vibrations of the slab, and decreases relatively quickly. This observation is also characteristic for missile impacts with hard missiles. The missile is slowed down completely to zero velocity as shown in Figure 24. The flight direction of the missile is reversed and it moves back again with a small velocity (see Figure 24).

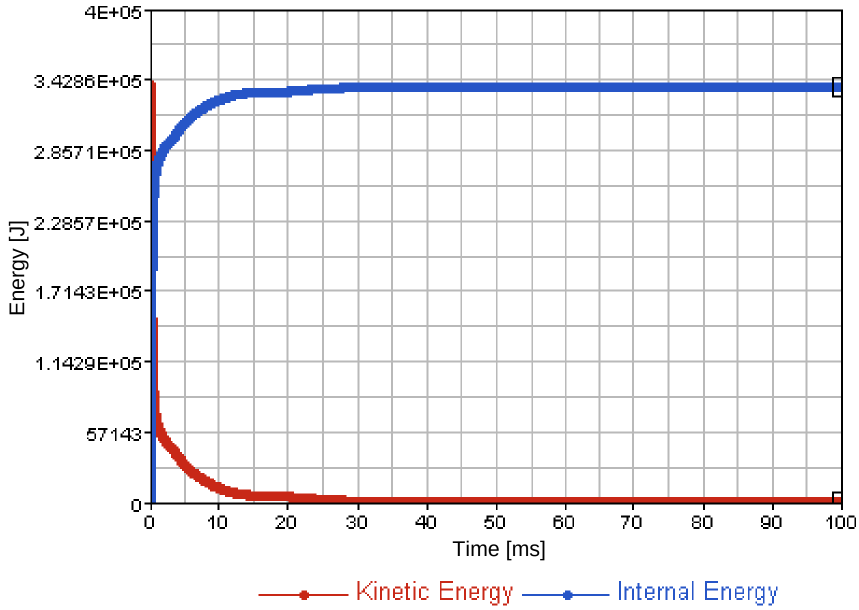

Fig. 22: Energy balance for the analysis on the VTT-CNSC-IRSN Punching Shear Test.

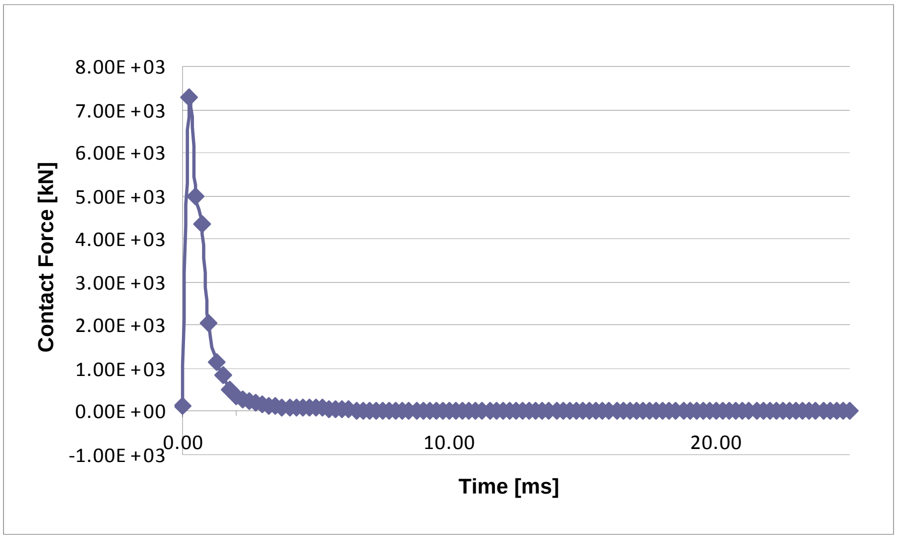

Fig. 23: Contact force versus time between missile and slab.

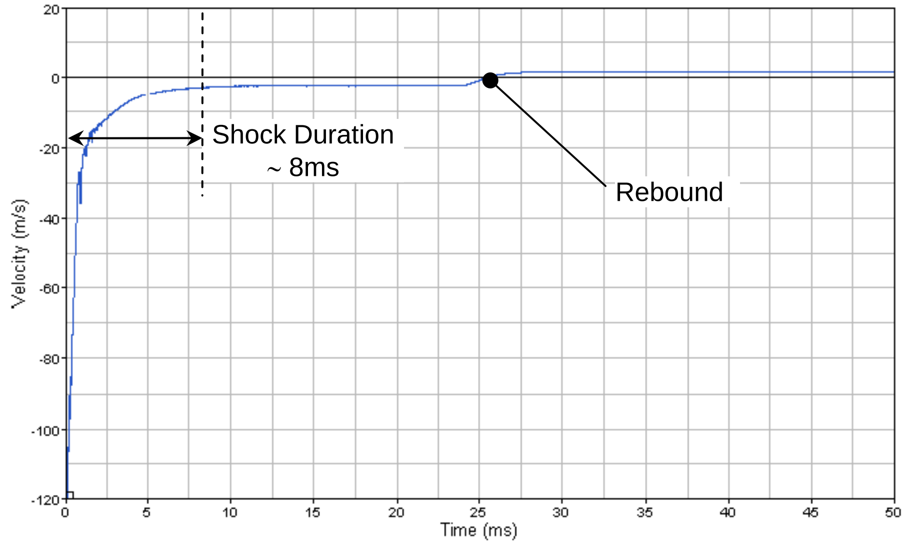

Fig. 24: Missile velocity versus time.

Figure 25 shows the damage on the front and back side of the reinforced concrete slab. The calculated residual penetration on the front side of the slab caused by the missile is 50mm. On the backside significant scabbing occurs, which is typical for punching shear tests.

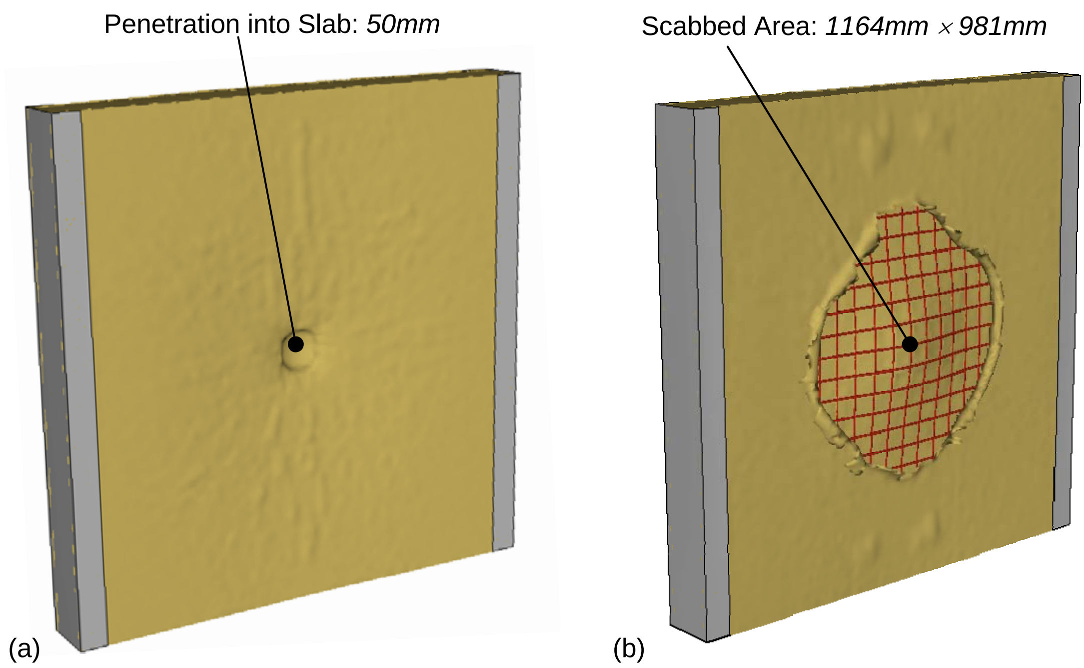

Fig. 25: Damage of the reinforced concrete slab after impact: (a) front side, (b) back side.

Figure 26 shows the simulated punching shear failure mechanism in more detail. During the impact process a shear cone develops and longitudinal cracks occur in the concrete (parallel to the front and back surface of the slab) around the impact zone indicated by a reduction in mass density. These cracks cause layers of concrete on the backside of the slab to fall of (scabbing). After the impact process the slab partly bounces back leading to a partly closure of cracks. However, a permanent (residual) deflection of the slab remains around the impact zone.

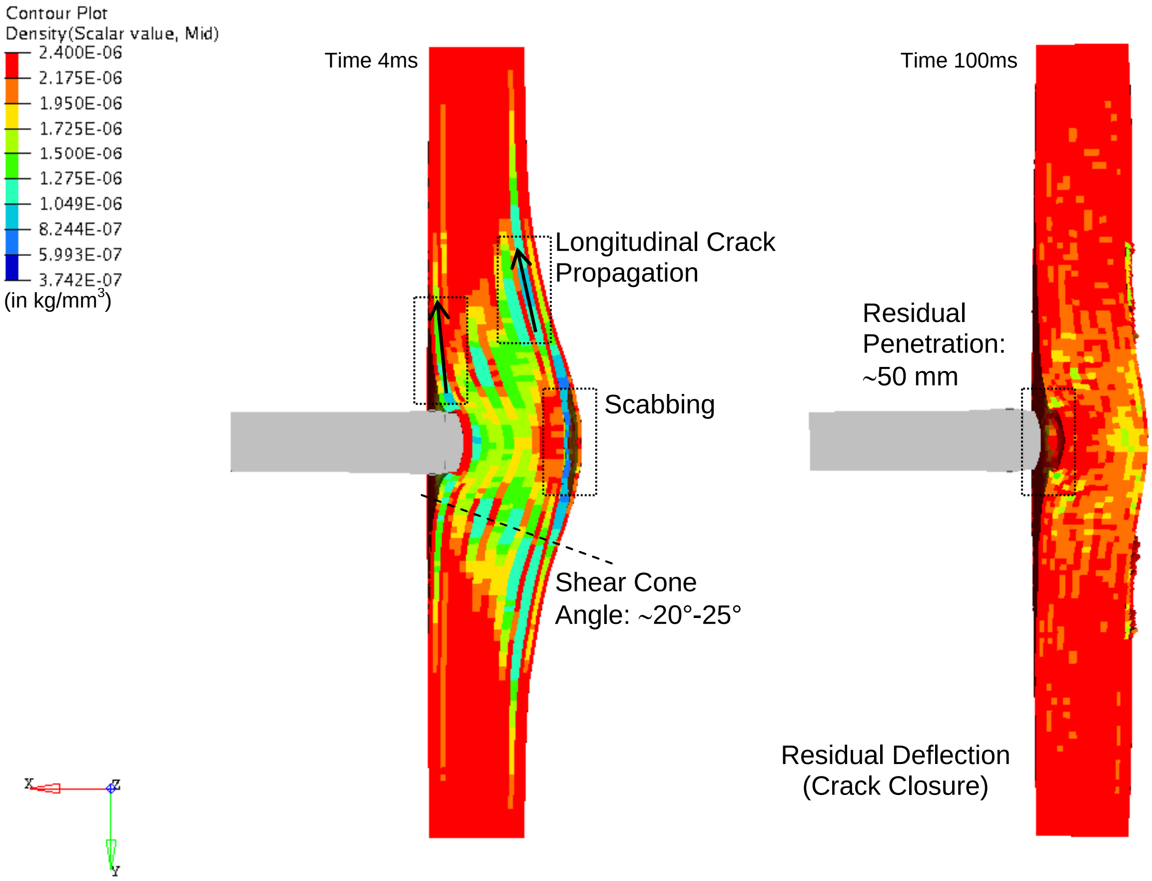

Fig. 26: Failure mechanism.

Figure 27 shows the deflection versus time of the rear reinforcement in the slab centre position. The deflection reaches its maximum rather quickly in the impact process and decreases smoothly to its residual level. The curve in Figure 27 shows no signs of larger vibrations, which is in agreement with the timely behaviour of the contact force between missile and concrete slab displayed in Figure 23. Figure 28 shows the plastic strain in the rebars, which indicates a slight local rupture of the front reinforcement in the impact zone.

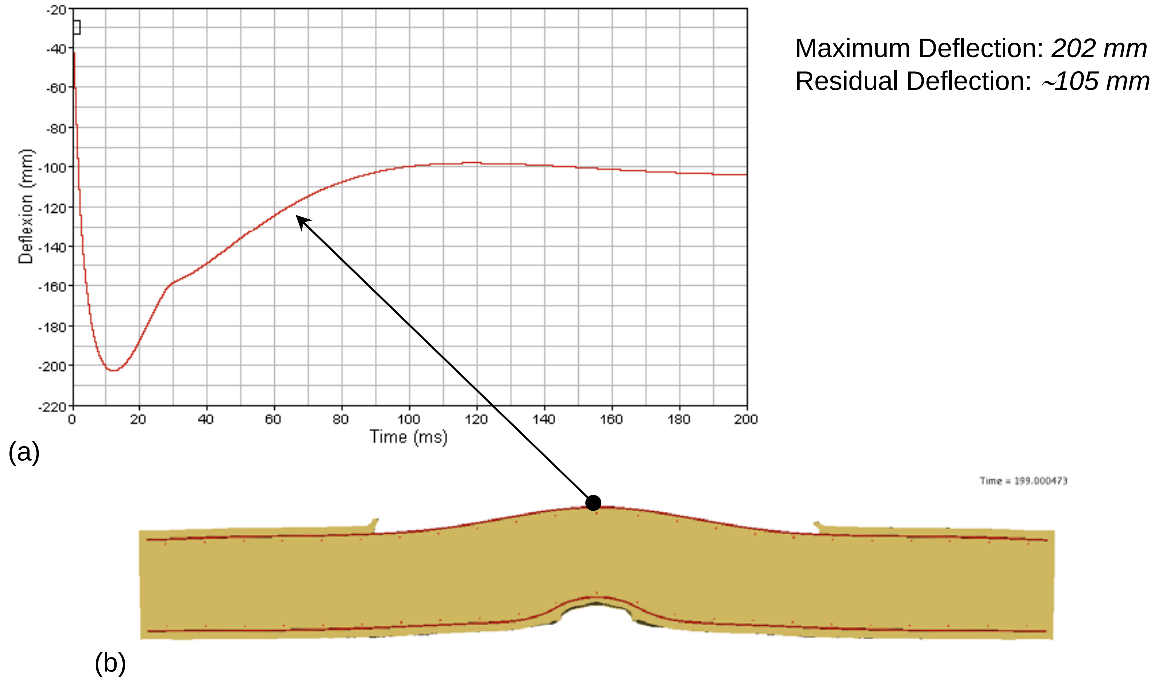

Fig. 27: (a) Deflection versus time at rear reinforcement at slab centre and (b) residual deformed shape.

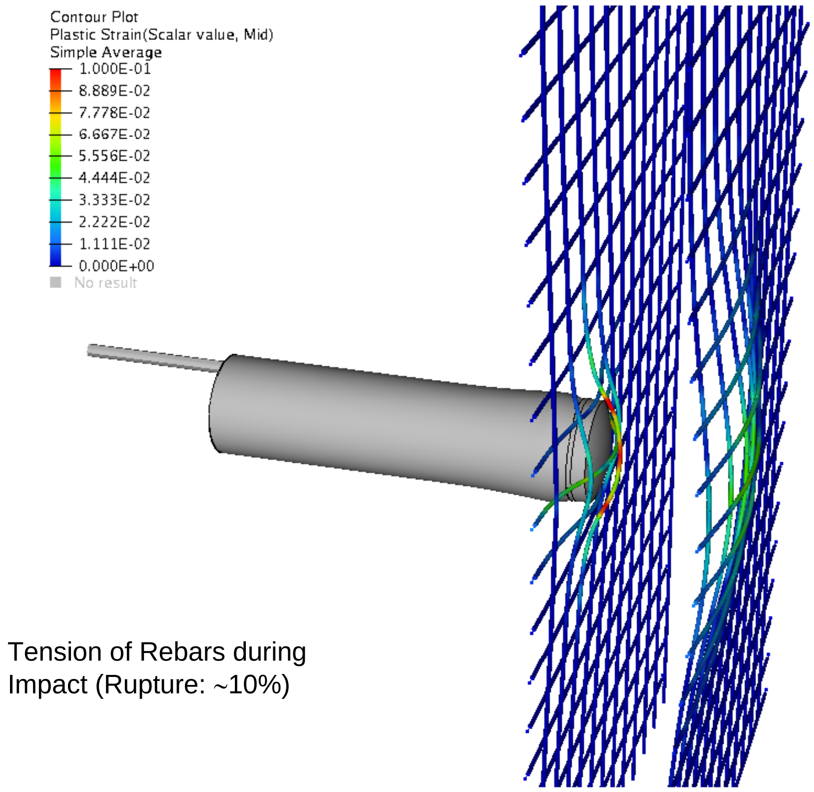

Fig. 28: Local damage of rebars.

6 Summary and Outlook

In this EUR report the FE modelling approach and results of analyses on the recently performed VTT-IRSN Flexural Tests and the VTT-CNSC-IRSN Punching Shear Tests using the explicit FE solver RADIOSS were described. The FE analyses were carried out within the Benchmark Project "Improving the Robustness of Assessment Methodologies for Structures impacted by Missiles (IRIS)" of the Subgroup on Concrete of the Working Group on the Integrity and Ageing of Components and Structures (IAGE) of the Nuclear Energy Agency (NEA).

A Lagrangian modelling approach was chosen for the missile and the concrete slab. The steel reinforcements inside the concrete slabs were modelled with beam elements with proper cross section definitions. Special emphasis was put on the constitutive modelling of all involved materials. A special Drucker-Prager/Cap model, the model of Han and Chen, was used to model the constitutive behaviour of the concrete. Isotropic elastic-plastic constitutive models with strain-rate dependencies, where applicable, were used for steel reinforcement and missile.

The analysis results on the VTT-IRSN Flexural Test resemble the outcome of a typical flexural test with a soft missile. The missile loses all its initial kinetic energy in a time frame between 20-30 ms and its front section crushes completely indicating that a huge portion of its initial kinetic energy ends up as damage (deformation) energy of the missile. The concrete slab shows the typical crack pattern for flexural tests and a shear cone forms out. The slab vibrates due to the impact of the missile as indicated by the calculated timely responses for the displacements of certain positions on the slab surface and the strains of certain sections of the slab reinforcement. The slab vibrations are also indicated by the calculated timely response of the contact force between missile and slab with significant oscillations in the beginning and stabilization later on.

The simulation results for the VTT-CNSC-IRSN Punching Shear Test resemble the outcome of a typical punching shear test when a hard missile impacts a concrete slab. The missile loses all its initial kinetic energy in less than 10ms indicating a hard impact. The missile only deforms slightly, where as the slab shows large deformations and significant scabbing indicating that most of the missile's initial kinetic energy ends up as deformation and damage energy of the concrete slab. Time responses for contact force between missile and slab and displacement of the slab centre on its back indicate no significant vibrations of the slab as a consequence of the impact, which is typical for an impact involving a hard missile. The slab reinforcement on the front side in the impact zone shows significant plastic strains indicating slight rupture of the reinforcement.

In summary the FE analyses give reasonable and sound results that are realistic in view of the individual missile and slab characteristics. Main analysis results concerning impact duration, deformation and damage of missile and slab, slab vibrations, etc… are physically sound. The results of the simulations clearly show that with today's available FE codes (and sufficient hardware) it is possible to predict the outcome of missile impact tests realistically. Nevertheless, more in-depth comparisons between test and analysis results need to be carried out. These will be performed when the corresponding test results are released within the IRIS Benchmark Project.

7 References

Altair Engineering, 2009. The RADIOSS Manual Version 10.0. Troy: Altair Engineering Inc.

Altair Engineering, 2010. *OECD-NEA Benchmark Project IRIS – Constitutive Modelling of Reinforced Concrete under high impact Loading using RADIOSS Explicit.* Altair Report no. ALTGM-3312-09. Antony: Altair Engineering France.

Bathe, K.J., 1990. *Finite-Elemente-Methoden*. 2nd ed. Berlin: Springer-Verlag.

Chen, W.F., 2007. Plasticity in Reinforced Concrete. 1st ed. Fort Lauderdale, FL: Ross Publishing Inc.

Gueraud, R., Sokolovsky, A., Kavyrchine, M. & Astruc, M., 1977. Study of the Perforation of Reinforced Concrete Slabs by Rigid Missiles – General Introduction and Experimental Study, Part 1, *Nuclear Engineering and Design*, 41, pp. 91-102.

Han, D.J. & Chen, W.F., 1985. A non-uniform hardening plasticity model for concrete materials. Mechanics of Materials, 4 (3-4), pp. 283-302.

IRSN, 2010. *Data for the VTT-CNSC-IRSN Tests: Punching Mode - Revision B*. Data material for IRIS Benchmark participants, 1st February 2010.

Lacy, J.M., Novascone, S.,R., Richins, W.D. & Larson, T.,K., 2008. A Method for Selecting Software for Dynamic Event Analysis II: The Taylor Anvil and Dynamic Brazilian Test. In: *Proceedings of the 16th International Conference on Nuclear Engineering (ICONE16)*, Orlando, FL, paper no. ICONE16-48816.

Li, Q.M., Reid, S.R., Wen, H.M. & Telford, A.R., 2005. Local impact effects of hard missiles on concrete targets. *International Journal of Impact Engineering*, 32, pp. 224-284.

Johnson, G.R. & Cook, W.H., 1985. Fracture Characteristics of three Metals subjected to various Strains, Strain Rates, Temperatures and Pressures. *Engineering Fracture Mechanics*, 21 (1), pp. 31-48.

Jonas, W., Meshkat, R., Riech, H. & Rüdiger, E., 1979. Experimental Investigations to determine the Kinetic Ultimate Bearing Capacity of Reinforced Concrete Slabs subject to Deformable Missiles. In: *Transactions of the 5th SMiRT Conference*, Berlin, paper no. 8/5.

Nachtsheim, W. & Stangenberg, F., 1982. Interpretation of Results of Meppen Slab Tests – Comparison with parametric Investigations, *Nuclear Engineering and Design*, 75, pp. 283-290.

Nachtsheim, W. & Stangenberg, F., 1983. Selected Results of Meppen Slab Tests – State of Interpretation, Comparison with Computational Investigations. In: *Transactions of the 7th SMiRT Conference,* Chicago, paper no. J8/1.

Riera, J.D., 1968. On the Stress Analysis of Structures subjected to Aircraft Impact Forces, *Nuclear Engineering and Design*, 8, pp. 415-426.

Rüdiger, E. & Riech, H., 1983. Experimental and Theoretical Investigations on the Impact of Deformable Missiles onto Reinforced Concrete Slabs. In: *Transactions of the 7th SMiRT Conference,* Chicago, paper no. J8/3.

Sugano, T. et al., 1993a. Local damage to reinforced concrete structures caused by impact of aircraft engine missiles – Part 1: Test program, method and results. *Nuclear Engineering and Design*, 140, pp. 387-405.

Sugano, T. et al., 1993b. Local damage to reinforced concrete structures caused by impact of aircraft engine missiles – Part 2: Evaluation of test results. *Nuclear Engineering and Design*, 140, pp. 407-423.

Appendix: Material Parameters

The following base units are used for the material parameters: Kg (mass), mm (length), ms (time), GPa (stress)

Table A1: Material parameters for concrete.

Material Parameter	Value
Initial mass density ρ [kg/mm^3] Concrete slab Light-weight concrete filling missile	 $2.37 \cdot 10^{-6}$ $1.42 \cdot 10^{-6}$
Young's modulus E [GPa]	31.0
Poisson ratio	0.2
Compressive Strength F_c [GPa]	0.058
Compressive Strength $F_c^{'}$ inter rebar [GPa]	0.232
Tensile strength ratio F_t / F_c	0.1
Biaxial strength ratio F_b / F_c	1.2
Confined strength ratio F_2 / F_c	4.0
Confining stress ratio S_0 / F_c	1.25
Tensile tangent modulus H_t [GPa]	-3.0
Maximum Strength	0.99999
Total failure strain [GPa]	10^{31}
Initial hardening parameter	0.5
Failure / Plastic Transition pressure	0.0
Uni-axial plastic modulus	224.7
Dilatancy factor at yield	0.1
Dilatancy factor at failure	0.1
Maximum volumetric compaction	-0.35
Proportional yield	-0.01933
Initial beginning of cap	-0.01933
Initial end of cap	-0.04640
Initial triaxial plastic modulus	6.2
Failure strain (scabbing, punching shear only)	0.5

Table A2: Material parameters for the steel reinforcement.

Material property	Value
Mass density ρ [kg/mm^3]	$7.8 \cdot 10^{-6}$
Young's modulus E [GPa]	210
Poisson ratio	0.3
Johnson-Cook parameter a [GPa]	0.598
Johnson-Cook parameter b [GPa]	1.5
Johnson-Cook parameter n	0.99
Johnson-Cook parameter c	0
Maximum stress [GPa]	0.7

Equation for the Johnson-Cook model:

$$\sigma = \left(a + b\varepsilon_p^n\right)\left(1 + c\ln\frac{\dot{\varepsilon}}{\dot{\varepsilon}_0}\right)$$

Table A3: Main material parameters for stainless steel sections of missile VTT-IRSN Flexural Test.

Material Parameter	Value
Mass density ρ [kg/mm^3] Stainless steel pipe Stainless steel end cap	 $7.91 \cdot 10^{-6}$ $7.84 \cdot 10^{-6}$
Young's modulus E [GPa]	205
Poisson ratio	0.3
Tensile damage strain ε_{t1}	0.06
Tensile damage strain ε_{t2}	0.07
Maximum plastic strain ε_{max}	2
Scale factors strain-rate dependency At 0 ms^{-1} At 10^5 ms^{-1}	 1 1.01

Table A4: Tabular stress-strain values for stainless steel sections of missile VTT-IRSN Flexural Test.

Plastic strain ε_P	**Total stress σ [GPa]**
0.0000	0.2200
0.0002	0.2689
0.0007	0.3075
0.0010	0.3267
0.0015	0.3427
0.0020	0.3532
0.0028	0.3631
0.0042	0.3746
0.0062	0.3857
0.0084	0.3949
0.0110	0.4035
0.0142	0.4132
0.0184	0.4233
0.0242	0.4377
0.0299	0.4529
0.0348	0.4672
0.0402	0.4812
0.0441	0.4902
0.0488	0.5012
0.0525	0.5088
0.0562	0.5165
0.0588	0.5222
0.0609	0.5300

Table A5: Material parameters for carbon steel sections of missile VTT-IRSN Flexural Test and dome of missile VTT-CNSC-IRSN Punching Shear Test.

Material property	**Value**
Mass density ρ [kg/mm^3] Pipe (Flexural) Rear plate (Flexural) Dome (Punching shear)	 $7.85 \cdot 10^{-6}$ $7.80 \cdot 10^{-6}$ $8.44 \cdot 10^{-6}$
Young's modulus E [GPa]	205
Poisson ratio	0.3
Johnson-Cook parameter a [GPa]	0.355
Johnson-Cook parameter b [GPa]	0.47
Johnson-Cook parameter n	0.2
Johnson-Cook parameter c	0
Maximum plastic strain ε_{Pmax}	0.22
Maximum stress σ_{max} [GPa]	0.555

Table A6: Material parameters for pipe and plate sections of missile VTT-CNSC-IRSN Punching Shear Test.

Material property	Value
Mass density ρ [kg/mm^3] Pipe Rear plate	 $7.85 \cdot 10^{-6}$ $8.66 \cdot 10^{-6}$
Young's modulus E [GPa]	205
Poisson ratio	0.3
Johnson-Cook parameter a [GPa]	0.355
Johnson-Cook parameter b [GPa]	0.47
Johnson-Cook parameter n	0.2
Johnson-Cook parameter c	0
Tensile damage strain ε_{t1}	0.22
Tensile damage strain ε_{t2}	0.24
Maximum plastic strain ε_{Pmax}	1.0
Maximum stress [GPa]	0.555

Table A7: Material parameters for aluminium pipe of missile VTT-CNSC-IRSN Punching Shear Test.

Material property	Value
Mass density ρ [kg/mm^3]	$2.7 \cdot 10^{-6}$
Young's modulus E [GPa]	61
Poisson ratio	0.33
Johnson-Cook parameter a [GPa]	0.09027
Johnson-Cook parameter b [GPa]	0.22314
Johnson-Cook parameter n	0.375
Johnson-Cook parameter c	0
Maximum plastic strain ε_{Pmax}	10^{30}
Maximum stress [GPa]	0.175

European Commission

EUR 24880 EN – Joint Research Centre – Institute for Energy
Title: Numerical Analyses on the Missile Impact Tests performed at VTT within the Benchmark Project IRIS - Modelling Approach & Preliminary Results
Author(s): Oliver Martin, Vincent Centro, Thierry Schwoertzig
Luxembourg: Publications Office of the European Union
2011 – 30 pp. – 21 x 29.7 cm
EUR – Scientific and Technical Research series – ISSN 1018-5593
ISBN 978-92-79-20664-1
doi:10.2790/3456

Abstract
In this EUR report the Finite element (FE) modelling approach and preliminary results of analyses on the recently performed VTT-IRSN Flexural Tests and the VTT-CNSC-IRSN Punching Shear Tests using the explicit FE solver RADIOSS are described. The FE analyses are carried out within the Benchmark Project "Improving the Robustness of Assessment Methodologies for Structures impacted by Missiles (IRIS)" of the Subgroup on Concrete of the Working Group on the Integrity and Ageing of Components and Structures (IAGE) of the Nuclear Energy Agency (NEA) of OECD. A Lagrangian modelling approach is chosen for the missile and the concrete slab. Special emphasis is put on the constitutive modelling of all involved materials. A special Drucker-Prager/Cap model, the model of Han and Chen, is used to model the constitutive behaviour of the concrete. Isotropic elastic-plastic constitutive models with strain-rate dependencies (where applicable) are used for steel reinforcements and missiles. The FE analyses give reasonable and sound results in view of the individual missile and slab characteristics. Main outcomes of the analysis concerning impact duration, deformation and damage of missile and slab, slab vibrations, etc… are physically sound. The results of the analyses clearly show that with today's available FE codes (and sufficient hardware) it is possible to predict the outcome of missile impact tests realistically. Nevertheless, more in-depth comparisons between test and analysis results need to be carried out when the test results are distributed to the benchmark participants.

How to obtain EU publications

Our priced publications are available from EU Bookshop (http://bookshop.europa.eu), where you can place an order with the sales agent of your choice.

The Publications Office has a worldwide network of sales agents. You can obtain their contact details by sending a fax to (352) 29 29-42758.

The mission of the JRC is to provide customer-driven scientific and technical support for the conception, development, implementation and monitoring of EU policies. As a service of the European Commission, the JRC functions as a reference centre of science and technology for the Union. Close to the policy-making process, it serves the common interest of the Member States, while being independent of special interests, whether private or national.

LD-NA-24880-EN-C

EUROPEAN COMMISSION

Publications Office

ISBN 978-92-79-20664-1